# Optimizing the Efficiency of Buoyancy Dynamics in Sea Wave Energy Conversion Using Up-Pumping method with Three Primary Buoy Shapes

**Nuwan Talawitage[1*], Sumira Ariyasinghe[1], Sampath Dissanayake[1], Wasantha Bandara[1], Chaminda Karunasena[1], Sumith Baduge[1], Nanditha Hettiarachchi[1], Gayan Kahandawa[2]**

[1]*Department of Mechanical and Manufacturing Engineering, Faculty of Engineering, University of Ruhuna, Sri Lanka*
[2] *Institute of Innovation, Science and Sustainability, Federation University, Churchill Campus, Australia*

*Corresponding author: nuwan.talawitage@gmail.com

DOI: 10.29322/IJSRP.14.07.2024.p15109

Paper Received Date: 14th May 2024
Paper Acceptance Date: 22nd June 2024
Paper Publication Date: 6th July 2024

**Abstract**
Harnessing the power of ocean waves holds great promise for sustainable electricity generation. There is abundant sea wave energy around Sri Lanka as an island nation. There are numerous sea wave energy harnessing techniques implemented around the world. This study delves into buoyancy-driven wave energy conversion systems, specifically focusing on the up-pumping method. We explored how different shapes of buoys—cylindrical, spherical, and cubical—can optimize energy capture. Additionally, we investigated how placing a steel buoyancy cover at different heights within each buoy affects performance.

Our experiments, conducted in a controlled lab setting with simulated waves, revealed clear differences in performance among the buoy shapes. The spherical buoy, especially when the cover was positioned lower down, stood out for its ability to convert wave motion into usable energy more effectively. This configuration enhanced the displacement of pressurized air, maximizing mechanical work output.

These findings are crucial for designing more efficient wave energy conversion technologies in future. By understanding how buoy shape and cover placement influence performance, we can develop systems that are not only more effective but also more reliable in harnessing coastal wave energy.

This research contributes valuable practical insights to the field of marine renewable energy, supporting efforts to transition away from fossil fuels toward sustainable alternatives.

**Keywords**: *buoyancy dynamics; ocean wave energy; up-pumping method; buoy shapes; energy conversion, sustainable energy solution; buoyancy; sea wave energy; sea wave generator.*

## 1. INTRODUCTION

A substantial percentage of the global electricity production comes from fossil fuels [1 2]. Because of its potential to enhance supply security, boost growth in economy, and reduce emissions of $CO_2$, there has been increasing attention in developing ocean energy technology and establishing ocean energy markets world-wide [1 3].The first generation of commercial ocean energy devices was introduced in 2008, and the first units installed were SeaGen in the UK and Pelamis in Portugal [1 4].

Being an island nation in the Indian ocean, Sri Lanka has a coastline of 1,340 km and territorial waters covering about 21,500 km² [1 5]. The contiguous zone reaches up to 24 nautical miles from the edge of the territorial zone, while the exclusive economic zone (EEZ) covers approximately 510,000 km² [1 5. With this background, Sri Lanka has a significant potential for ocean energy, which can be harnessed utilising five distinctive technologies: tidal rise and fall (barrages), tidal/ocean currents, waves, temperature gradients, and salinity gradients [1 2].

Numerous methods have been analyzed globally to generate electricity from sea waves. Our experiments lay on identifying the most efficient and cost-effective approach to convert sea wave energy into electricity. Sea waves contain significant usable energy in the forms of potential and kinetic energy. Our aim is to harness this energy using a mechanical system, specifically the up-pumping method. Kinetic energy manifests in various ways, which can potentially damage the structural integrity of the system.

Therefore, we plan to design our system to mitigate such damage while maximizing energy extraction by efficiently optimizing the shape of the buoy. The optimal buoy shape has better hydrodynamic performance [6].

Basically, in the up-pumping method, we pump water to a higher position tank and then use a conventional hydropower system, to produce electricity. In this paper, we will not describe the up-pumping method in detail. Instead, we will focus on testing the harnessing of energy from sea waves using an optimal buoy shape. Sea waves exhibit a large range of energy. However, because each pump has a maximum stroke, we cannot utilize the full range of wave energy as it may damage our buoy system. Therefore, we aim to provide a consistent wave environment for our buoy system by using a wave breaker and stabilizing the buoy's vertical movement with a buoyancy cover. This approach is intended to achieve better hydrodynamic performance while ensuring the safety of the mechanical system.

## 2. LITERATURE REVIEW

Prior to introduce Sea Water Up-pumping technique, we searched literature for systems used in world to convert the wave power to electricity.

### *a) Wave energy conversion technologies*

#### *Oscillating Water Column*

Various Oscillating Water Column (OWC) devices have been suggested over time. Depending on their proximity to the coastline, OWC devices can be categorized as either fixed or floating (Figure 01) [7 8]. Fixed OWCs are typically mounted on the shoreline or nearby, often utilizing natural or man-made structures like breakwaters and rock cliffs [8 9]. Installing WECs directly on the shoreline offers a number of advantages, including simplified maintenance operations that reduce relative costs, minimized expenses for the mooring system, and the installation of all electrical equipment for energy conversion externally to water [7 8].

OWC devices are intended to generate vertical water oscillation within a chamber, creating alternating compression and expansion of air in the chamber. Due to the continuous change in airflow direction, conventional horizontal-axis air turbines are unsuitable. Alan Arthur Wells of Queen's University of Belfast developed the Wells turbine in the midst of 1970s to address this issue [7]. The Wells turbine is a low-pressure air turbine that can rotate in one direction regardless of airflow direction. Its blades feature symmetrical airfoils, with the symmetry plane matching the plane of rotation.

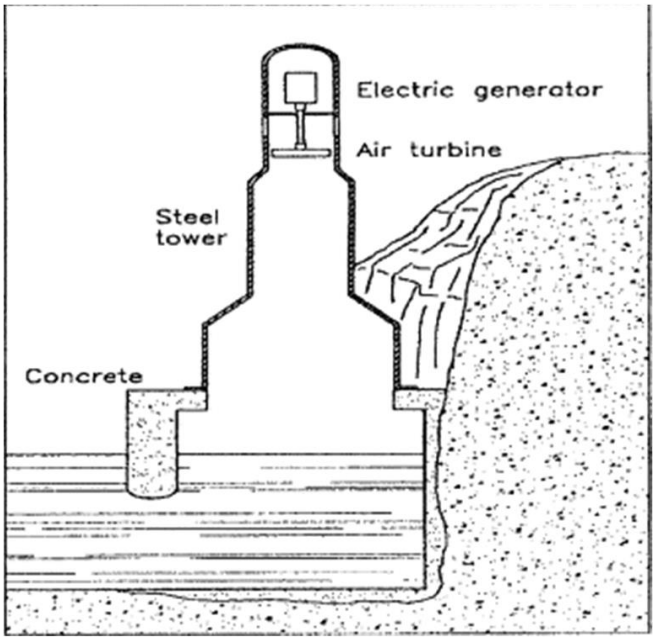

*Figure 01; Sectional Drawing of a OWC plant [8]*

The other category of OWC devices consists of floating systems, which operate on the same principle as fixed OWCs. The primary distinction lies in the structure where the OWC device is mounted. The most common solution involves using floating buoys with chambers designed to generate water oscillation.

Yoshio Masuda's team in Japan, developed one of the earliest floating OWCs during the 1960-70s. This system, known as the Backward Bent-Duct Buoy (BBDB), features a floating buoy anchored to the seabed and a L-shaped chamber was used [8 10].

*Wave-Activated Body*

The category of Wave-Activated Bodies (WAB) includes a number of solutions for harnessing sea wave energy. These systems typically consist of two or more components designed to generate relative motion, thereby driving the energy converter [8 11].

WAB systems are usually intended for nearshore or offshore installation to take advantage of the more consistent waves found in open seas, as opposed to those near the coastline. However, placing these systems far from the shore introduces several challenges. Transferring the energy collected by the WECs to the mainland, was done by long underwater cables or pipes. Additionally, a robust mooring system is necessary to withstand extreme weather conditions [8 12].

Given the variety of WABs, a classification based on the working principle of the device is introduced [8 9]. This classification includes single-body heaving buoys (Figure 02), two-body heaving systems, fully submerged heaving systems (Figure 03), pitching devices, bottom-hinged systems, and many-body systems.

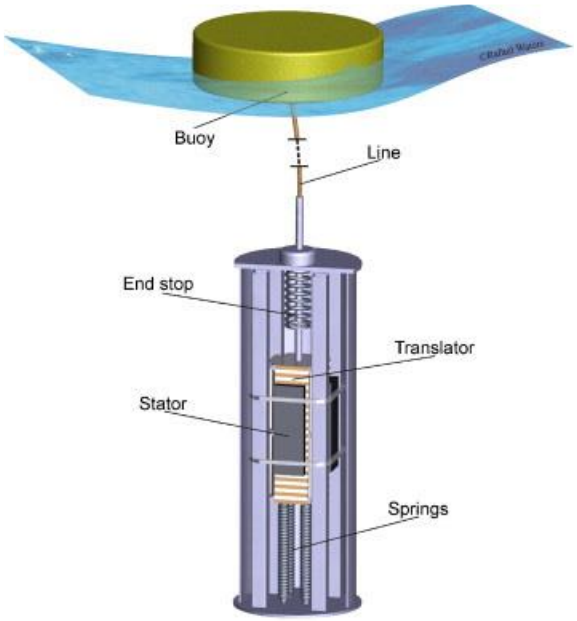


*Figure 02; Working Principal of a Single-body heaving buoys [8] in Lysekil project in Norway [9]*

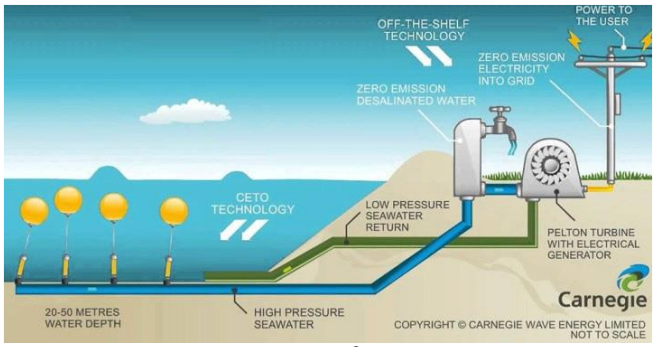


*Figure 03; Working Principal of Fully submerged heaving system [8]. CETO 6 project in Australia. However, the CETO 6 project was discontinued on 31 October 2019 [13 14].*

*Pitching Device*

In these devices, the main motion is produced by a relative rotation between the parts [8]. Salter's Duck is an example which was developed by Salter's study at the University of Edinburgh between the 1970-80s. This device features a cam-shaped floater [15 16]. Initially, a hydraulic pumping system was planned to convert the rotary motion into electricity, later followed by a gyroscope system [8 16].

Pelamis was a well-known example for pitching device (Figure 04) )[8 9]. This pitching device developed by the Scottish company Pelamis Wave Power Ltd., was first tested in Orkney, Scotland, between 2004-07, and a wave farm with three devices was installed in Portugal in 2008 [9]. The device, consisting of four cylindrical buoys connected by hinged joints, was designed to pump oil at high pressure into accumulators to drive hydraulic motors coupled with induction generators, achieving a rated power of 750 kW [17 18]. Despite its initial promise, technical failures led to the wave farm's shutdown after two months, causing financial difficulties for the

company. The intellectual property was later transferred to the Scottish government in late 2014. The Pelamis concept has since been revived in other projects aiming to optimize the system's geometry for better energy harvesting [8 19].

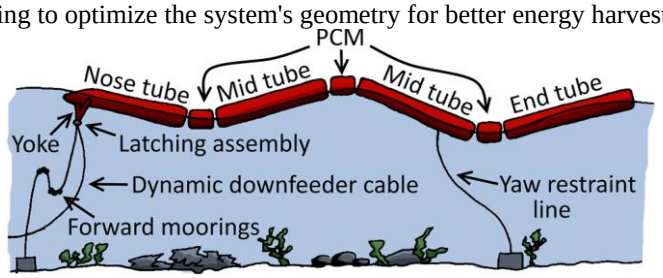


*Figure 04; Working Principal of Pelamis [8]*

*Bottom-Hinged Systems*

The bottom-hinged systems are designed for the purpose of exploiting sea waves in shallow water (10-15m), where the sea motion is mainly horizontal [8].

Oyster is an example for this type of Wave Energy Converter (WEC) (Figure 05), developed by Whittaker's et al at Queen's University of Belfast and tested by Aquamarine Power at the European Marine Energy Centre's Billia Croo test site in Orkney. The Oyster consists of a barrier with five horizontally stacked cylinders, fixed by a horizontal hinge. The motion of breaking waves causes the barrier to rotate, activating a high-pressure pump that sends high pressure water to the coastline, where hydro turbines and alternators generate electricity [20 21].

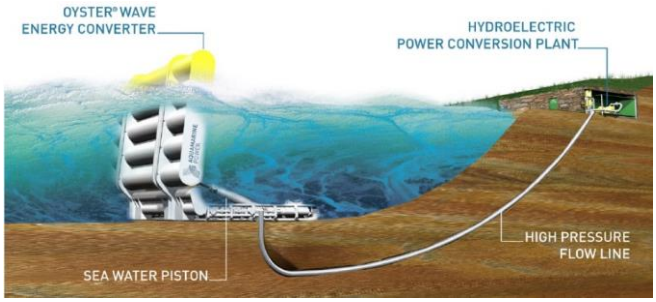


*Figure 05; Working principal of Oyster [8]*

*Many-Body System*

Wavestar is an example of a many-body system (Figure 06) [9]. The initial tests on this device began by Niels and Keld Hansen (2000), in Denmark. A small-scale prototype (1:40) was studied (2004) at the laboratory of Aalborg University. A grid-connected small-scale (1:10) pilot plant was installed at Nissum Bredning in 2005. Later on, in 2009, a 1:2 scale prototype was connected to the grid in Hanstholm. The plant was dismantled in 2013 [22]. Similar to other systems described previously, Wavestar utilizes the relative rotation of the buoys to pump oil at high pressure and drive hydraulic motors [07]. There are ongoing research is underway on a full-scale version of the device. As shown in Figure 06, Wavestar consists of 20 buoys (10 m diameter), arranged in two lines, capable of extracting up to 6 MW depending on the climatic conditions of the North Sea. The system can also be assembled in a star shape, using 60 buoys to achieve a total rated power of 18 MW [8 22 23].

Figure 06; Wavestar [8]

*Overtopping Devices*

Overtopping devices (OD) harness sea waves by converting the kinetic energy of water into potential energy, which is then used by a low-head hydro turbine. This process involves creating an artificial water reserve at a level higher than sea level and using a ramp to channel sea waves into the reserve.

One of the earliest OD pilot plants was built in 1985, called Tapered Channel Wave Power Device (Tapchan) in Norway [9 24]. It featured a collector carved into a rocky cliff, with a 60-meter-wide entrance, lifting water into a reservoir 3 meters above ocean level and covering 8500 m². A low-head Kaplan-type hydro turbine with a rated power of 350 kW converted this potential energy into electricity. The plant was destroyed by a storm in 1988 and decommissioned in 1991[8].

An example of an offshore OD is the Wave Dragon, built by Wave Dragon Aps in Denmark. A 20 kW prototype (scale 1:4.5) was installed and studied in Nissum Bredning fjord in 2003 [25]. This floating device has a water reserve refilled by sea waves using two reflectors and a ramp, which converts kinetic energy into potential energy. Kaplan turbines then use this energy to generate electricity. The system must be moored to the seabed and oriented towards the wave direction [9 26].

The Seawave Slot-Cone Generator is another OD designed for onshore installation. It consists of three chambers at different heights, each with an opening at the top. An external ramp increases the water height, filling the internal chambers. A multistage low-head hydro turbine converts the potential energy into electricity. Plans for installations along the west Norwegian coast have yet to be realized [8 27 28].

The OIST Wave-Energy Project also falls under this category. It channels breaking waves into a duct to run a low-head hydro turbine. Initial tests in 2016 led to the installation of two half-scale devices (35 cm wide turbine, 1.3 kW) in the Maldives in 2018, accumulating over 7200 hours of operation in ten months. In 2018, two full-scale WECs (60 cm turbine, 8 kW peak) were installed operating for over 2000 hours in three months [8 29].

## 3. EXPERIMENTAL DESIGN

a) Design and fabricating a sea wave generator

We need to use a wave generator primarily because we require a constant wave amplitude to maintain consistent wave energy during our experiments, which is challenging to achieve in the unpredictable conditions of the real sea. Hydraulic model experiments are essential for understanding maritime structure design, but scale effects must be managed, especially for studies involving sand beds or wave impact forces.

The details of the sea wave generator we used are as follows: the channel had a height of 600 mm, a width of 300 mm, and a length of 5400 mm. We determined the optimal practical wave that closely resembles a real sea wave and maintained these conditions throughout our experiment. The wave had a wave period of 4 seconds, a wavelength of 1600 mm, and a height of 100 mm.

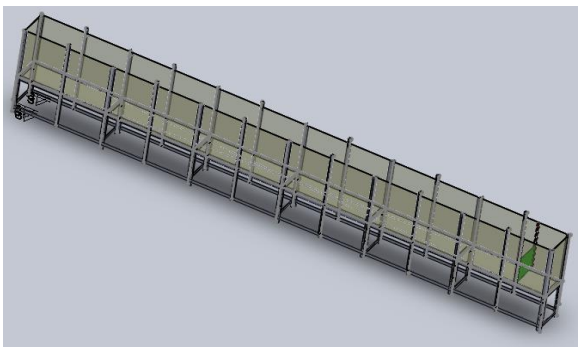

Figure 7: 3D model of sea wave generator

We designed a Back wave breaker (Figure 8) to prevent shock loads on the front wall and the formation of back waves, which could interfere with the generated waves. We incorporated a wave breaker made of Perspex, extending up to the maximum water level, and this reduces the power of both the generated waves and the back waves.

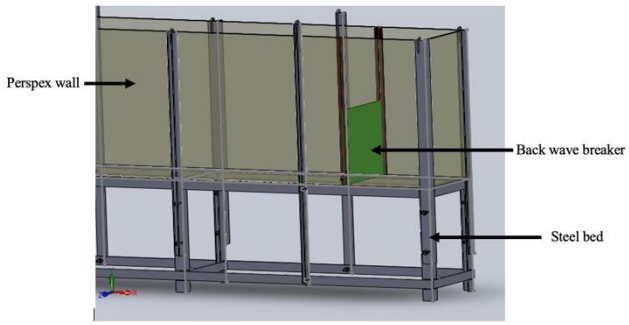

Figure 8: Back wave breaker


Figure 9: Fabricated sea wave generator

b) Design considerations and development of the model

The design and developing of the model is the most significant part of the project, requiring considerable time and effort to finalize from numerous potential designs. In many global projects, common issues considered were large systems requiring high investments, failure to test models in actual conditions, structures designed for offshore installation causing added difficulties, and lack of consideration for continuous electricity generation.

We selected the up-pumping method due to its benefits, including minimal cost, durability, and ease of production for domestic electricity. Unlike many methods where pumps are submerged beneath the sea, our design places the pump above the sea. This approach helps to minimize corrosion and simplifies maintenance. In regions where the water depth is greater than half the wavelength, the wave energy flux is calculated using the following equation;

$$P = \frac{\rho g^2}{64\pi} H_{m0}^2 T \approx \left(0.5 \frac{\mathrm{kW}}{\mathrm{m}^3 \cdot \mathrm{s}}\right) H_{m0}^2 \, T,$$

with,
P = the wave energy flux per unit of wave-crest length
$H_{m0}$ =the significant wave height
T =the wave period,
ρ =the water density
g =the acceleration by gravity.

This equation shows that wave power is proportional to the wave period and to the square of the wave height. When the significant wave height (in meters), and the wave period (in seconds), the result is the wave power in kilowatts (kW) per meter of wave front length.

Based on the data from Unawatuna area, the minimum wave height is 1 meter, the mean wave period is 4 seconds and the mean number of waves 7 per minute; the mean potential wave energy per minute per 1 meter can be calculated as follows:

Mean potential wave energy per minute = 0.5

Mean potential wave energy per minute,$(0.5x1^2x4)$ =2kW

Total coastline of Sri Lanka (Km) = 1700

Considering the total coastline of Sri Lanka, which is 1,700 km

Mean potential wave power of Sri Lanka (1700×1000×2) =3,400 MW

We aimed to address these concerns effectively, and after selecting the up-pumping approach, we focused on designing the model. With rapidly changing amplitudes and directions of the sea waves, and particularly in unpredictable sea conditions, especially during bad weather, our model must be robust and capable of efficiently absorbing wave energy. We considered these parameters in our design.

Our group embarked on a detailed design process, starting with drafting and hand-sketching models, which were then fabricated and tested in real sea conditions at Unawatuna, Sri Lanka. Initial tests revealed errors, leading to multiple iterations and modifications. Through this rigorous process, we developed a final design (Figure 10) that prioritizes simplicity, stability, and efficiency. The design leverages buoyancy to drive a piston pump, minimizing energy losses by avoiding complex components like hinges and bearings. It robustly withstands external forces such as drag, lift, and pressure, focusing on z-direction force to ensure stability and durability. A steel cover protects the buoyancy system from shock loads, enabling it to handle large wave amplitudes. This final model effectively addresses wave energy conversion challenges, resulting in a robust and efficient system.

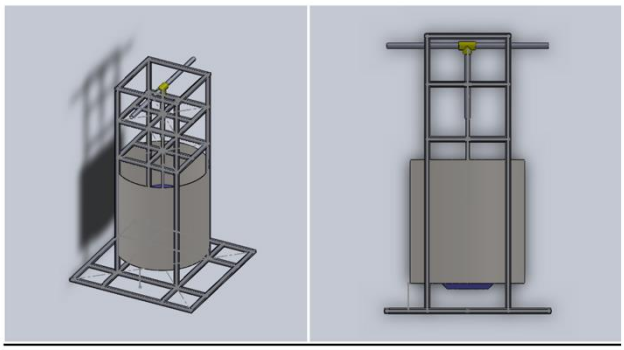


Figure 10: 3D model of the Final Design of the Model

*c) Selection of the pump, valve, and utilization of the buoyancy steel cover*

In designing the pump (Figure 11), we focused on several key factors: the pump must handle a higher head, resulting in higher back pressure, the strokes are intermittent, and the material used must minimize corrosion. Considering these requirements, the most suitable choice is a Reciprocating Piston Pump. Therefore, we bought a double-acting pneumatic cylinder from the local market and modified as its work for our requirement.

We utilized two non-return valves: one as a foot valve and the other as an output valve. These valves may introduce small local losses.

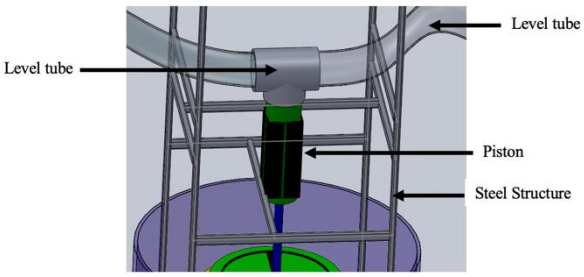


Figure 11: Final 3D Design of the Pump

A steel cover for the buoyancy (figure 12) was designed to prevent horizontal forces from acting on it, absorb these forces, and transfer them to the structure. This allows the buoyancy to move smoothly up and down. We used galvanized steel sheets for the buoyancy cover, which is adjustable with nuts and bolts according to our experimental requirements.

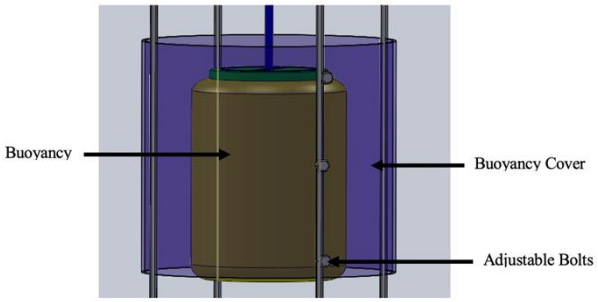


Figure 12: Steel buoyancy Cover

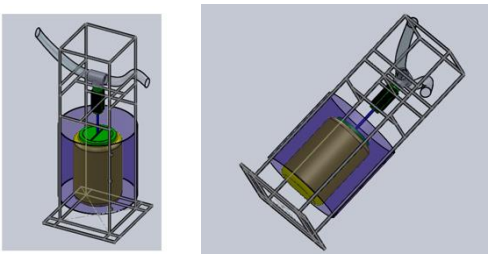

Figure 13 Final 3D Design of the model

Considering all the factors mentioned above, we finalized the design of our model using SOLIDWORKS. The comprehensive design addresses the critical requirements for efficient wave energy conversion while ensuring durability and stability in challenging marine environments.

*d) Fabrication of the model*

*Steel Structure*

We utilized 1/4-inch flat irons for the structure. The base of the structure is designed to support variable loads and withstand shock loads from waves. The central part of the model has a specialized design to accommodate the pump and system. Additionally, the model is designed to secure pipes and valves at the top.

*Pump and Buoyancy*

The pump, the most critical component of the model is imperative to ensure there are no leakages in the piston. The joint between the piston rod and buoyancy must be robust because all forces acting on the buoyancy are transmitted to that joint. The items used to fabricate the pump and buoyancy are: Plastic container available in the local market, Two non-return valves, double-acting pneumatic cylinder, pneumatic tubes, and pneumatic joints (Figure 14).


Figure 14: The fabricated pump

Table 1: Specifications of Pump

| Data | Value |
|---|---|
| Brand | Airtec |
| Type | Double acting cylinder |
| Cylinder bore | 18mm |
| Piston stroke | 20cm |
| Maximum out flow per stroke | 50ml |

The bottom outlet was left open to air flow, while the top outlet was connected to the non-return valves using a pneumatic T-joint, as shown in the figure 14. A special device, referred to as a connector, was fabricated to attach the buoyancy to the piston rod, as illustrated in Figure 15.After this modification, no leakage was observed.

Three types of buoyancies (cylindrical, sphere and cubic shapes) were fabricated for testing:
Each shape was designed and fabricated to have the same cross-sectional area since force is equal to pressure multiplied by area.

The buoyant force on an object submerged in a fluid is given by Archimedes' principle, which states:

*Buoyant Force=Volume of displaced fluid×Density of the fluid×Acceleratio*

Mathematically, this is:
$F_b=V\times\rho\times g$

where:

V = the submerged volume of the object
ρ =the density of the fluid
g =the acceleration due to gravity

*Buoyant Force and Pressure:*

The buoyant force can also be understood in terms of pressure differences at different depths. Consider a submerged object: The pressure at the bottom of the object is higher than the pressure at the top due to the increase in pressure with depth in a fluid.

The net upward force (buoyant force) is due to this pressure difference.

Let's denote:

- A as the cross-sectional area of the submerged object.
- $h_t$ and $h_b$ as the depths of the top and bottom surfaces of the object, respectively.
- $P_t$ and $P_b$ as the pressures at the top and bottom surfaces of the object, respectively.
- $Pb=\rho\, g\, h_b$ and $P_t=\rho\, g\, h_t$ due to hydrostatic pressure.
-

The force at the bottom is

$F_b = P_b \times A = (\rho\ g\ h_b) \times A$

The force at the top is:

$F_t = P_t \times A = (\rho\ g\ h_t) \times A$

The net buoyant force is the difference between these forces:

$F_{buoyant} = Fb - Ft = (\rho g h_b) \times A - (\rho g h_t) \times A = \rho g A (h_b - h_t)$

Therefore, we designed and fabricated our buoyancies (figure 16) to match the cross-sectional area of cylindrical, cubical, and spherical shapes equally. This ensured accuracy of results while maintaining all other variables constant.

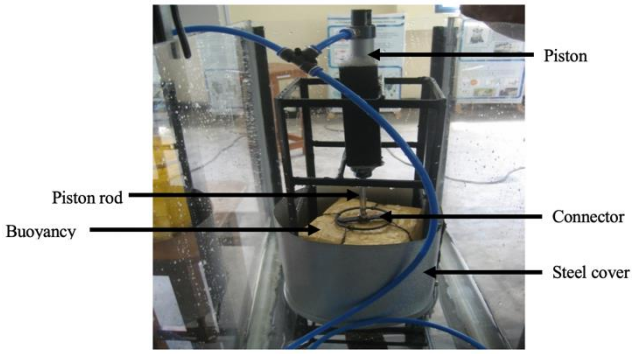


Figure 15: Fabricated Model

Figure 16: Designed and Fabricated Spherical and Cubic Shaped Buoyancy

e) Testing

After fabricating our model and sea wave generator, we conducted laboratory testing under two main conditions: changing the positions of the buoyancy covers, with 8 different positions available as shown in the figure 17, and changing the shape of the buoyancy, with three different shapes cylindrical, spherical, and cubical available.

*Changing Steel Buoyancy Cover position:*

We adjusted the position of the galvanized steel buoyancy cover by first marking the structure to specify the positions of the cover, as illustrated in the following figure 17.

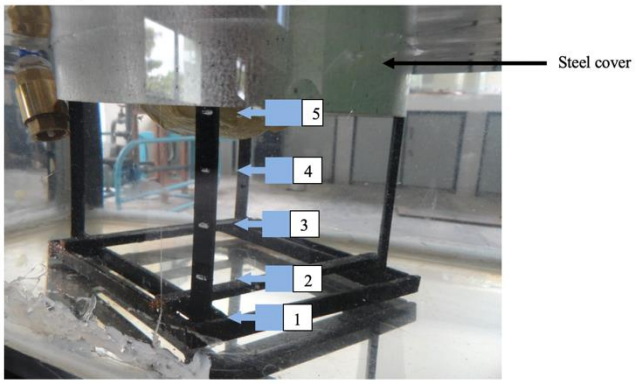


Figure 17: Testing positions of the steel buoyancy cover

*Changing Buoyancy shape:*

We changed the shape of the buoyancy and did testing for each type of buoyancy. We used three types of buoyancies, Cylindrical, Spherical and Cubical shapes.
We aimed to maintain a consistent cross-sectional area of 25600 square millimetres. Our cylindrical buoyancy used a diameter of 180 mm and height of 180 mm, while our spherical buoyancy had a diameter of 180 mm, and our cubical buoyancy had a side length of 160 mm. These dimensions resulted in approximately the same cross-sectional area of 25600 square millimetres. We adapted readily available items from the local market for our buoyancy solutions. Since exact measurements were not provided, we adjusted them using waterproof adhesive tape to achieve our desired values.

We tested our three shapes of buoyancy under the same conditions. During our measurements, we generated a wave with a period of 4 seconds, a wavelength of 1600 mm, and a height of 100 mm. Practically, to achieve these wave characteristics, we maintained a constant wave height of 100 mm. The paddle moved at a speed of 400 mm/s with an interval of 4 seconds between movements.

We used a stopwatch to measure the time and collected water for 3 minutes, calculating the flow rate by dividing the collected volume by 3. We repeated this process five times for each position of the buoyancy cover. We used a 500 ml graduated cylinder with 5 ml increments to measure the water volume. Finally, we determined the flow rate for each specific position of the buoyancy cover, rounding the values to the nearest 5 ml to ensure clarity and ease of distinction when presenting our results.

## 4. RESULTS

Table 2, 3, and 4 consequently presents our findings on the Flow rates of the Cylindrical, Spherical and Cubical shapes in different cover positions. Figure 18, 19, and 20, visually represents the Flow rates of the Cylindrical, Spherical and Cubical shapes in different cover positions.

Table 2: Flow rates of the Cylinder shape in different cover positions

| Cover Position | Flow Rate (millilitres per minute) |
|---|---|
| 1 | 55 |
| 2 | 100 |
| 3 | 70 |
| 4 | 60 |
| 5 | 55 |
| 6 | 30 |
| 7 | 25 |
| 8 | 25 |

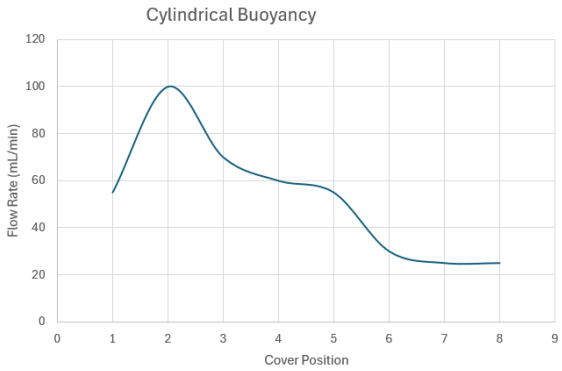


Figure 18: Flow rate vs. buoyancy cover positions for the cylindrical buoyancy shape.

Table 3: Flow rates of the Spherical shape buoyancy in different cover positions

| Cover Position | Flow Rate (millilitres per minute) |
|---|---|
| 1 | 100 |
| 2 | 100 |
| 3 | 95 |
| 4 | 100 |
| 5 | 105 |
| 6 | 120 |
| 7 | 110 |
| 8 | 95 |

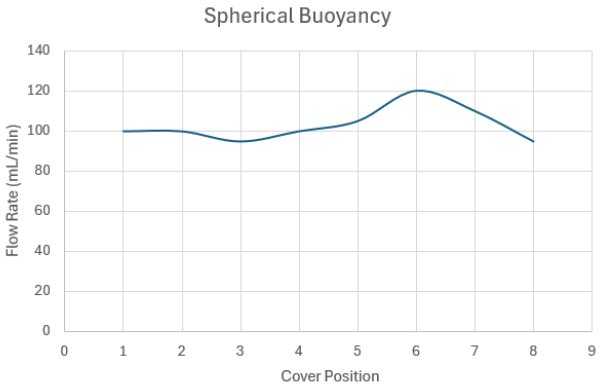


Figure 19: Flow rate vs. buoyancy cover positions for the spherical buoyancy shape.

Table 4 : Flow rates of the Cubical shape buoyancy in different cover positions

| Cover Position | Flow Rate (millilitres per minute) |
|---|---|
| 1 | 60 |
| 2 | 85 |
| 3 | 100 |
| 4 | 90 |
| 5 | 85 |
| 6 | 80 |
| 7 | 75 |
| 8 | 75 |

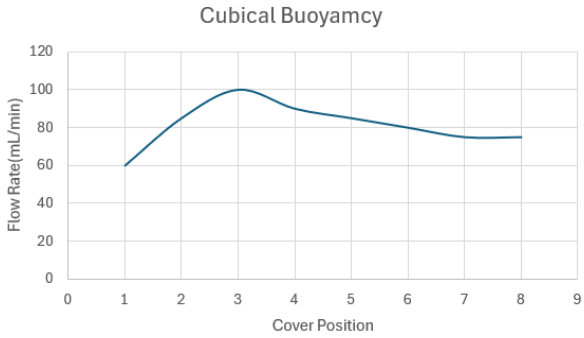


Figure 20: Flow rate vs. buoyancy cover positions for the cubical buoyancy shape.

## 5. DISCUSSIOIN

Our primary objective was to determine the optimal buoyancy shape for the up-pumping method. Additionally, we aimed to identify the best cover position for the buoyancy. To ensure the accuracy of our results, we maintained all other parameters constant and applied consistent conditions during our measurements.

To simulate wave conditions, we generated waves with a wave period of 4 seconds, a wavelength of 1600 mm, and a height of 100 mm. These parameters were chosen to closely match real sea wave conditions at Unawatuna, Sri Lanka, using our available wave generator. To achieve a wavelength of 1600 mm, the paddle moved at a speed of 400 mm/s, creating waves with a 4-second interval between movements to maintain a period of 4 seconds. We used a self-adhesive measuring tape on the wave generator wall to measure and maintain a wave height of 100 mm and wavelength of 1600mm.

We measured the flow rate by collecting water in a beaker for 3 minutes and using a stopwatch for timing. The flow rate was calculated by dividing the collected volume by 3. This process was repeated five times for each position of the buoyancy cover. To ensure clarity and ease of distinction, we rounded the flow rate values to the nearest 5 ml when presenting our results.
We used a 500 ml graduated cylinder with 5 ml increments to measure the water volume. Although the least count was 5 ml, collecting water for 3 minutes and repeating the steps five times for each position helped reduce the error in our readings.

*Summary of Findings:*

Cylindrical Shape: The flow rates varied significantly across different cover positions, with the highest flow rate observed at position 2 (100 ml/min) and the lowest at positions 7 and 8 (25 ml/min).
Spherical Shape: This shape exhibited more consistent flow rates across cover positions, with the highest at position 6 (120 ml/min) and the lowest at position 8 (95 ml/min).
Cubical Shape: The flow rates showed moderate variation, with the highest at position 3 (100 ml/min) and the lowest at positions 7 and 8 (75 ml/min).
The data suggest that the spherical shape demonstrated the most consistent performance across different cover positions, indicating it may be the most efficient shape for the up-pumping method under the tested conditions. The cover positions significantly influenced the flow rates, highlighting the importance of optimizing this parameter for each buoyancy shape.

## 6. CONCLUSIONS

In this study, we investigated the optimal buoyancy shape for the up-pumping method and the best cover position for the buoyancy. We tested three different shapes—cylindrical, spherical, and cubical—under controlled conditions, maintaining a consistent wave energy and other experimental parameters to ensure accurate and comparable results.

Our experiments revealed that the spherical buoyancy shape demonstrated the most consistent performance across various cover positions. Specifically, the spherical shape achieved a relatively stable flow rate, with the highest flow rate recorded at position 6 (120 ml/min). In contrast, the cylindrical and cubical shapes showed greater variability in their flow rates, indicating a stronger dependency on the cover position.

The findings suggest that the spherical shape is the most efficient for the up-pumping method under the conditions tested, as it maintained higher and more stable flow rates compared to the other shapes. Additionally, our results highlighted the importance of optimizing the cover position to maximize the efficiency of the buoyancy system.

In conclusion, the spherical buoyancy shape, combined with an optimal cover position, appears to be the best choice for enhancing the efficiency of the up-pumping method. Further research is recommended to explore different wave conditions, additional buoyancy shapes, and variations in cover design to confirm and extend these findings for practical applications.

References

1. Thennakoon TMTN, Hewage HTM, Sandunika DMI, et al. Harnessing the power of ocean energy: A comprehensive review of power generation technologies and future perspectives. . *J Res Technol Eng* 2023;4(3):73-102.
2. Melikoglu M. Current status and future of ocean energy sources: A global review. *Ocean Engineering* 2018;148:563-73. doi: https://doi.org/10.1016/j.oceaneng.2017.11.045
3. Magagna D, Uihlein A. Ocean energy development in Europe: Current status and future perspectives. *International Journal of Marine Energy* 2015;11:84-104. doi: https://doi.org/10.1016/j.ijome.2015.05.001
4. Esteban M, Leary D. Current developments and future prospects of offshore wind and ocean energy. *Applied Energy* 2012;90(1):128-36.
5. Arachchige GM, Jayakody S, Mooi R, et al. A review of previous studies on the Sri Lankan echinoid fauna, with an updated species list. *Zootaxa* 2017;4231(2):zootaxa.4231.2.1. doi: 10.11646/zootaxa.4231.2.1 [published Online First: 20170209]
6. Ge W, Ji S, Jin Y, et al. Optimization of Buoy Shape for Wave Energy Converter Based on Particle Swarm Algorithm. *Applied Sciences* 2024; 14(5).
7. Rusu E. Evaluation of the Wave Energy Conversion Efficiency in Various Coastal Environments. *Energies* 2014; 7(6).
8. Curto D, Franzitta V, Guercio A. Sea Wave Energy. A Review of the Current Technologies and Perspectives. *Energies* 2021; 14(20).
9. Aderinto T, Li H. Ocean Wave Energy Converters: Status and Challenges. *Energies* 2018; 11(5).
10. Masuda Y, Yamazaki T, Outa Y, et al. Study of Backward Bent Duct Buoy. *OCEANS '87* 1987:384-89.
11. Vicinanza D, Margheritini L, Kofoed JP, et al. The SSG Wave Energy Converter: Performance, Status and Recent Developments. *Energies* 2012; 5(2).
12. Yemm R, Pizer D, Retzler C, et al. Pelamis: experience from concept to connection. *Philos Trans A Math Phys Eng Sci* 2012;370(1959):365-80. doi: 10.1098/rsta.2011.0312
13. Alfarsi H. CETO System: Clean Electricity and Water Desalination Using Ocean Waves. Profolus. , 2021.
14. ARENA. Carnegie CETO 6 Technology, 2021.
15. Falnes J. A review of wave-energy extraction. *Marine Structures* 2007;20(4):185-201. doi: https://doi.org/10.1016/j.marstruc.2007.09.001
16. Renewable_Energy. Salter's Nodding Duck., 2019.
17. Thomson RC, Chick JP, Harrison GP. An LCA of the Pelamis wave energy converter. *The International Journal of Life Cycle Assessment* 2019;24(1):51-63. doi: 10.1007/s11367-018-1504-2
18. Wikipedia. Pelamis Wave Energy Converter, 2021.
19. Wang LG, Ringwood JV. Control-informed ballast and geometric optimisation of a three-body hinge-barge wave energy converter using two-layer optimisation
. *Renew Energy* 2021;171:1159–70.
20. Evans P. Oyster Ocean Power System to Provide 1 GW by 2020, 2021.
21. Poenaru V, Scurtu IC, Dumitrache CL, et al. Review of wave energy harvesters. *Journal of Physics: Conference Series* 2019;1297(1):012028. doi: 10.1088/1742-6596/1297/1/012028
22. WAVESTAR. Energy Innovation Cluster, 2021.
23. NeoZone. Wavestar, la centrale électrique qui utilise la houle pour produire de l'énergie, 2021.
24. Ecthelion. Norwave Wave Power Plant
, 2021.
25. Frigaard P, Kofoed JP, Knapp W. Wave Dragon: wave power plant using low-head turbines. International Conference and Exhibition on Small Hydropower. Hidroenergia, 2004.
26. Kofoed JP, Frigaard P, Friis-Madsen E, et al. Prototype testing of the wave energy converter wave dragon,. *Renewable Energy* 2006;31(2):181-89.
27. Cascajo R, García E, Quiles E, et al. Integration of Marine Wave Energy Converters into Seaports: A Case Study in the Port of Valencia. *Energies* 2019; 12(5).
28. Buccino M, Banfi D, Vicinanza D, et al. Non Breaking Wave Forces at the Front Face of Seawave Slotcone Generators. *Energies* 2012; 5(11).
29. Shintake T. OIST Wave Energy Project, 2021.